

## THREE-DIMENSIONAL P-WAVE CRUSTAL VELOCITY STRUCTURE BENEATH ATHENS REGION (GREECE) USING MICRO-EARTHQUAKE DATA

G. DRAKATOS, N. MELIS, V. KARASTATHIS, G. PAPADOPOULOS,  
D. PAPANASTASSIOU, G. STAVRAKAKIS  
*National Observatory of Athens, Institute of Geodynamics, Athens, Greece*

### Abstract

Three-dimensional P-velocity structure of the upper crust was determined by inversion of P-wave travel times in the Athens broader area (Greece), where a destructive earthquake of 5.9 Ms magnitude occurred on September 7, 1999. The investigated area is located at the eastern part of Greek mainland and was previously considered as a region of low seismicity. To investigate the 3-D crustal structure of the region a two-step tomography procedure has been applied. The selected data set consists of 240 located earthquakes, recorded by at least eight stations of a portable ten station network, which was installed in the area by the Institute of Geodynamics, immediately after the main event. In order to improve the initial velocity model, before the inversion of the travel times, the "minimum 1-D" initial velocity model was obtained. The results show that at shallow depths low velocities are predominant in the investigated region, without any sharp horizontal velocity variation. The low velocities at this depth seem to be typical for sedimentary basins, like those of the investigated region. The most predominant feature is a low velocity layer at a depth of 6–8 km. At the same depth, few aftershocks have been recorded by the local network. At deeper layers, higher velocities cover the central part of Attiki region, almost coinciding with the transition zone between the Pelagonian and Attico-Cycladic massifs.

### 1. Introduction

The Athens broader region is located at the Attiki Prefecture, at the eastern part of the Greek mainland Figure 1(a) and has been considered as an area of low seismicity. Few strong earthquakes have been reported in the adjacent area surrounding Athens [1, 2, 3, 4, 5, 6,] in historical times (1705, 1805 and 1889). The largest of them occurred in 1705 (38.2°N, 23.8°E) with estimated magnitude about  $M=6$  [7]. Ambraseys [3] after a detailed investigation concludes, that "The historical seismicity record for Athens appears to have been almost free of destructive earthquakes".

Nevertheless, on 7 September 1999 the most catastrophic earthquake of the last century in Greece occurred. In fact, it is the first moderate-to- strong shock ( $M_s = 5.9$ , 11:56:50.5 GMT) ever reported to have occurred at such a small epicentral distance ( $D = 18$  km) from the historical center of the city. Moreover, it is the first shock in the long history of Athens to cause casualties within its urban area [7]. Using P-wave polarities from the permanent network of the Institute of Geodynamics and those provided by other networks, the focal mechanism solution was determined. The solution indicates that the main shock rupture is associated with normal faulting. The nodal planes have parameters NP1 (strike/dip/rake): (293/51/-90); NP2 (strike/dip/rake): (113/39/-90) [8], while the determined seismic moment and fault radius are  $M_0 = 7.13 \times 10^{24}$  dyn.cm and  $R = 9.39$  km, respectively [9].

Immediately after the 7<sup>th</sup> September earthquake, the Institute of Geodynamics (National Observatory of Athens), installed an array of 10 portable analog stations in the vicinity of the main shock in order to monitor the aftershock activity. The network operated for two months and more than 1500 aftershocks have been recorded. A first attempt to estimate the spatial and temporal characteristics of the aftershock sequence was made by several investigators [6, 9, 11,12, 13].

The lack of local networks in Attiki region did not allow up to day the investigation of the three-dimensional crustal structure of Athens urban area. Only few information exist from tomography studies of regional scale [14, 15, 16, 17, 18, 26]. In the present study, based on the data of the local network, the 3-D crustal velocity structure of the area is investigated and therefore, the first accurate velocity model for the region is derived.

## 2. Geological and Seismotectonic Regime

The study region is located on the western margin of the Attico-Cycladic massif. Attiki has a complex geological structure. Its northern part consists of the non-metamorphic formations of the Pelagonian geotectonic zone, while its southern part belongs to the Attico-Cycladic massif. The dominant tectonic feature is the overthrust between these two units, trending NE – SW, composed of three successive thrust faults [19]. The basement rocks in the active region are Paleozoic shales and sandstones in altered phylites and quartz conglomerates, Triassic-Jurassic crystalline limestones, dolomites and a few outcrops of Cretaceous limestones and possibly Paleocene flysch of the Pelagonian zone. Neogene formations overlie uncomfortably the basement formation, while Quaternary deposits are unconsolidated sandy-clayed soils, talus cones and scree.

The Attiki region displays moderate neotectonic activity [19, 20]. The epicentral region is located between two important graben structures, the Corinthian Gulf to the west and Euboikos Gulf to the northeast (Figure 1(b)), which both are characterized by high seismic activity. Two main basins exist in the region. The Thriassio basin to the west and the Athens basin, which is developed between the mountains of Penteli, Parnitha and Aegaleo and is filled with neogene and Quaternary deposits (Figure 1(b)). The recent

seismic history of the area, does not indicate any previous significant seismic activity in the specific area, where the main shock was located.

### 3. Method

In order to investigate the three-dimensional crustal velocity structure of the region, the two-step tomography procedure proposed by Kissling *et al.* [21] has been applied.

As a first step, the travel time data are jointly inverted to obtain a 1-D velocity model, together with revised hypocenter coordinates and station corrections. This model is called the "minimum 1-D model" [22].

As a second step, the 3-D tomographic inversion is determined using the minimum 1-D model (Figure 2) as the starting model. In this step, the tomographic technique initially introduced by Thurber [23] and later improved by Eberhart-Phillips [24, 25] was applied. The method performs an iterative simultaneous inversion for 3-D velocity structure and hypocenter parameters using travel time residuals from local earthquakes.

The velocity of the medium is parameterized by assigning velocity values at the intersections (grid points) of a non-uniform, three-dimensional grid. The spacing within the grid is defined by trying to have enough ray paths near each grid point so that its velocity may be well resolved. The spacing need not be uniform throughout the study area. The velocity for a point along a ray path and the velocity partial derivatives are computed by linearly interpolating between the surrounding grid points. Thus, the solution will show gradual velocity variations rather than the sharp discontinuities shown in typical refraction models or block-type parameterizations. As a ray tracing technique, the approximate ray tracing proposed by Thurber [23] is used. This technique selects the ray paths as the arc with the fastest travel time out of a suite of circular arcs connecting the source and receiver. This is a very useful technique that performs very well for station to source distances less than 100 km [23, 24, 25], and is therefore the most suitable to be applied in the case of Athens broad region.

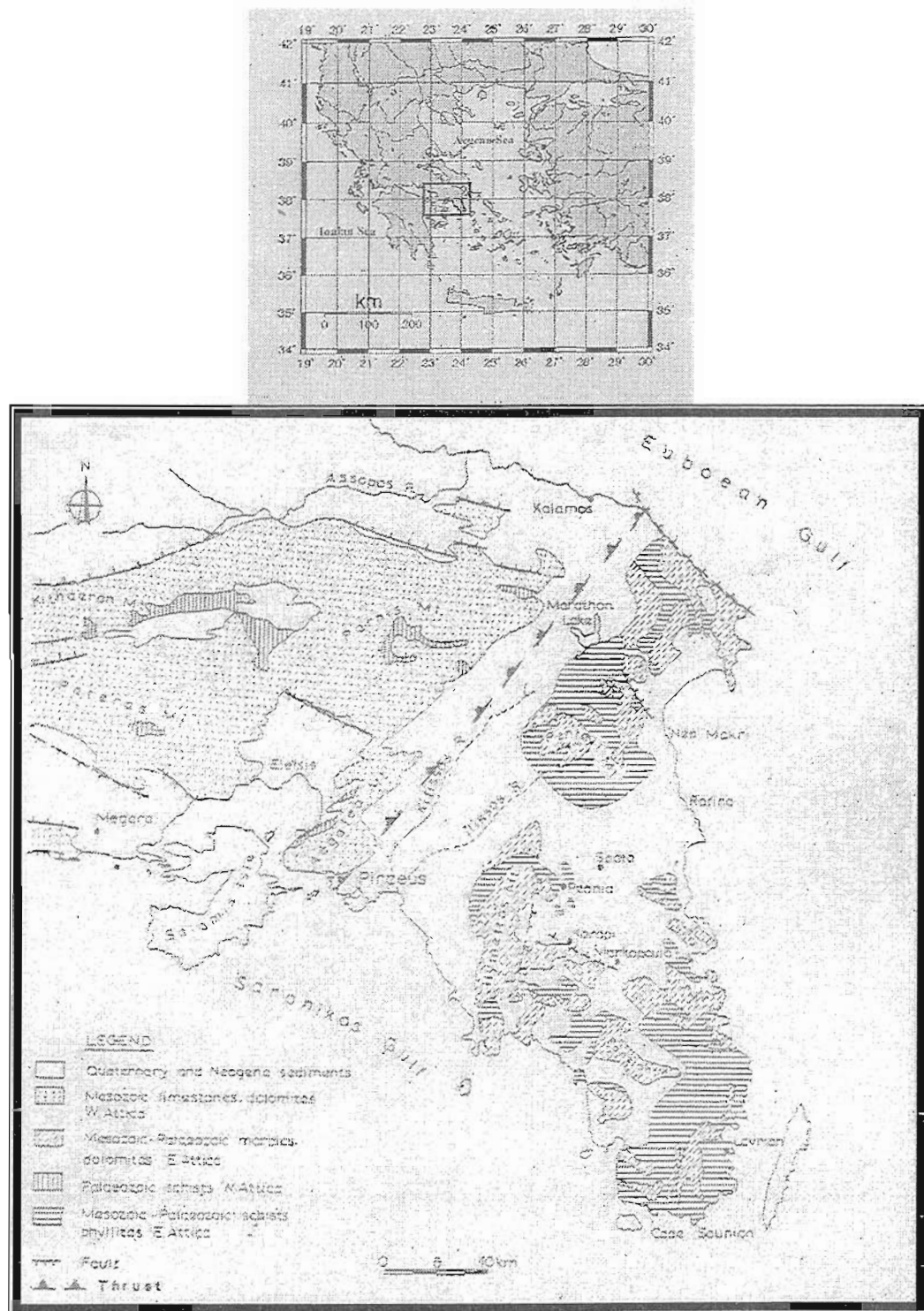


Figure 1. The location map of the investigated region (a) is shown, as well as a simplified geological and tectonic map of Attiki region (after Drakatos *et al* [27]). All symbols are explained in the attached legend.

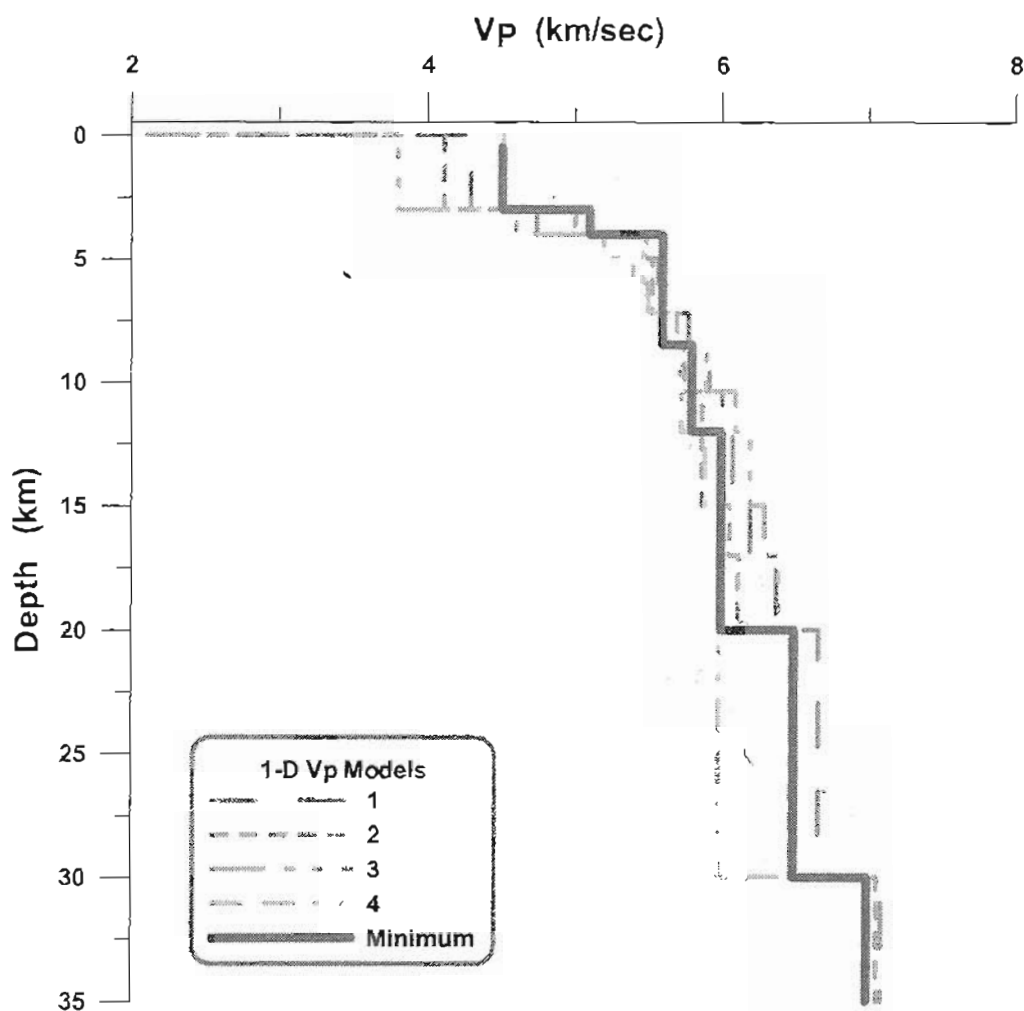


Figure 2. The minimum 1-D model used in this study is shown.

#### 4. Tomography Data and Results

The resolution and the reliability of the tomographic results strongly depend upon the degree of intersection of crossing rays. This presumes a dense station network with good distribution all over the investigated area. In order to overcome this difficulty, a "quality sensitive" spatial filtering technique was applied, following Drakatos *et al* [26]. For this purpose the list of all events located at the study area is sorted in decreasing order of number of phases, time and depth. The first event in the list is considered to be the center of a cube with specific dimensions. The list of events is processed sequentially and all the events lying within the cube are removed. When this step is completed, the second event in

the list is considered as the center of a new cube and the whole procedure is repeated on the last event.

So, from an initial data set consisting of more than 1500 local earthquakes, the final data set consists of the arrival times of 240 very well located earthquakes (Figure 3) each one of them recorded by at least 8 stations of the network.

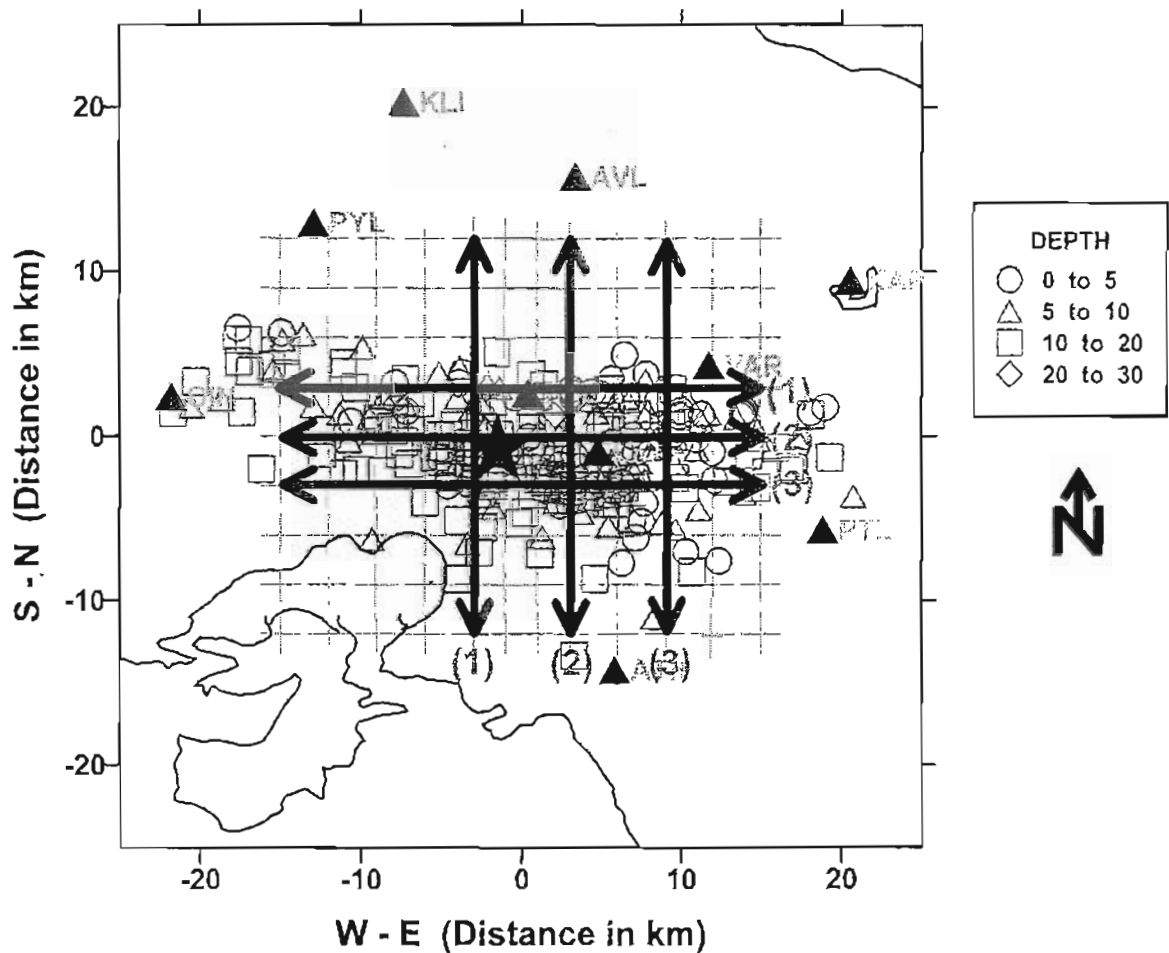


Figure 3. The map of the investigated region is shown.

- i) the star indicates the epicenter of the main shock
- ii) the open circles represent the aftershocks used in this study
- iii) the broken lines indicate the grid of nodes, where velocity is calculated
- iv) solid lines represent the cross-sections, in N-S and E-W directions.

For the implementation of the method, a set of nodes has been considered, in the area between  $37.8^{\circ}\text{N} - 38.5^{\circ}\text{N}$  and  $23.2^{\circ}\text{E}-24.0^{\circ}\text{E}$ , distributed in seven horizontal layers at a depth of 2, 4, 6, 8, 10, 12 and 15 km. Each grid consists of 12 nodes in the E-W and 9 nodes in the N-S direction, respectively. The distance between two consequent nodes is 3km in both EW and NS direction. The initial velocity values assigned at each horizontal plane of nodes are 4, 4.7, 5.1, 5.5, 5.9, 6.1 and  $6.4 \text{ km s}^{-1}$ , respectively. The velocity model used is the "minimum 1-D model", which has been obtained following the procedure proposed by Kissling *et al.* [21]. The damping factor assigned to the velocity during the inversion procedure was set to be 15%.

The total number of observations used is 2348. Some of the events are located outside the modeled area. The inclusion of earthquakes and (or) stations outside the modeled area (tomography box) is necessary to improve the ray path distribution within the modeled area. If only events and stations within the modeled area were included, the quality of hypocenter location and resolution of velocity would be significantly reduced. However, it must be remembered in interpreting the results that the peripheral velocity grid-points include ray paths from the surrounding area.

Before the inversion procedure, the relocation of events has been made. In order to achieve the best depth determination, we included in the relocation step except the P-wave arrival times and the S-wave arrivals too. The data set has been inverted five times to get a stable solution.

In order to detect any slight lateral variation of the velocity, after the first inversion the whole grid configuration was shifted to the NE by 3 km. The inversion procedure was performed again. Therefore, in Figures 4 and 5 the results of the inversion are shown, in terms of velocity perturbation at each node, after superposition of the two grids and only for the well resolved layers. To check the reliability and the stability of the solution, the number of hits at each node is calculated. The resolution and hence the reliability and the stability of the solution strongly depend upon the degree of intersection of crossing rays. This presumes a dense station network with good distribution all over the investigated area. Despite the relatively low number of stations, the number of hits is high, due to the fine distribution of the selected events and the small area of the investigated region. As a result, a large number of crossing rays passes from the grid points where the velocity values are calculated. The results are shown in Figure 6.

## 5. Discussion–Conclusions

The 3-D P-wave velocity structure of the upper crust of the Athens broader region is determined by inversion of the P-arrival times of local earthquakes. For the first time, a reliable 3-D velocity model is determined for the Attiki region. Due to the small extent of the investigated region, no sharp velocity variations were expected.

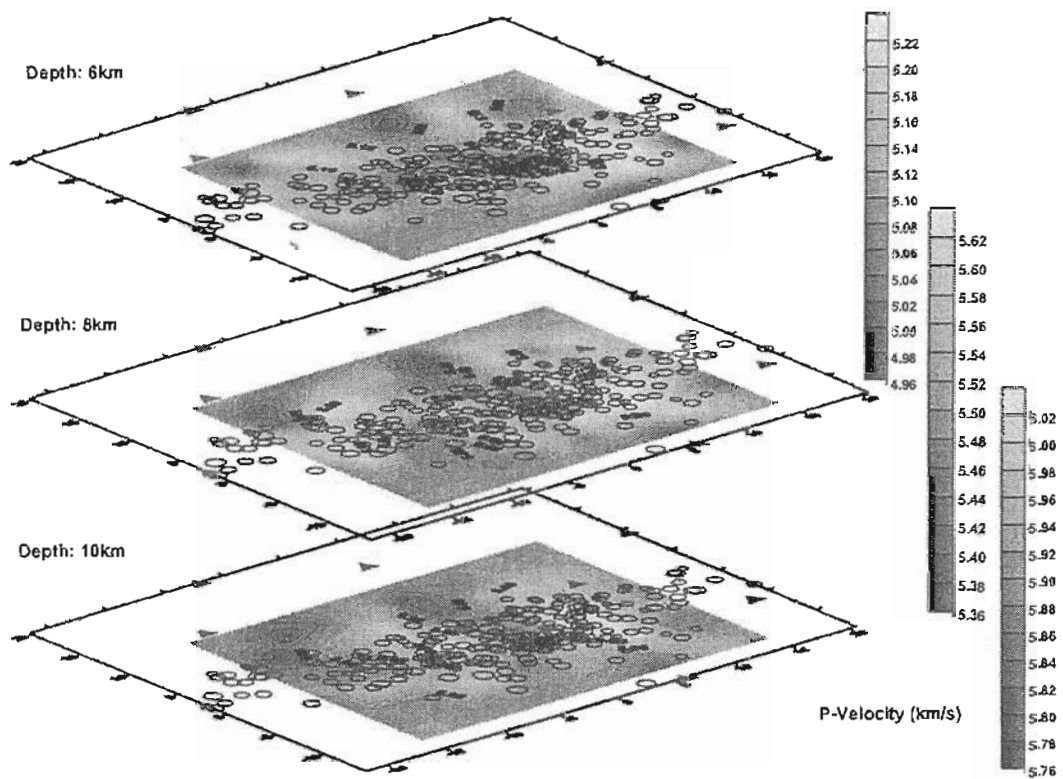


Figure 4. The 3-D P-wave velocity is shown, for the three well-resolved layers.



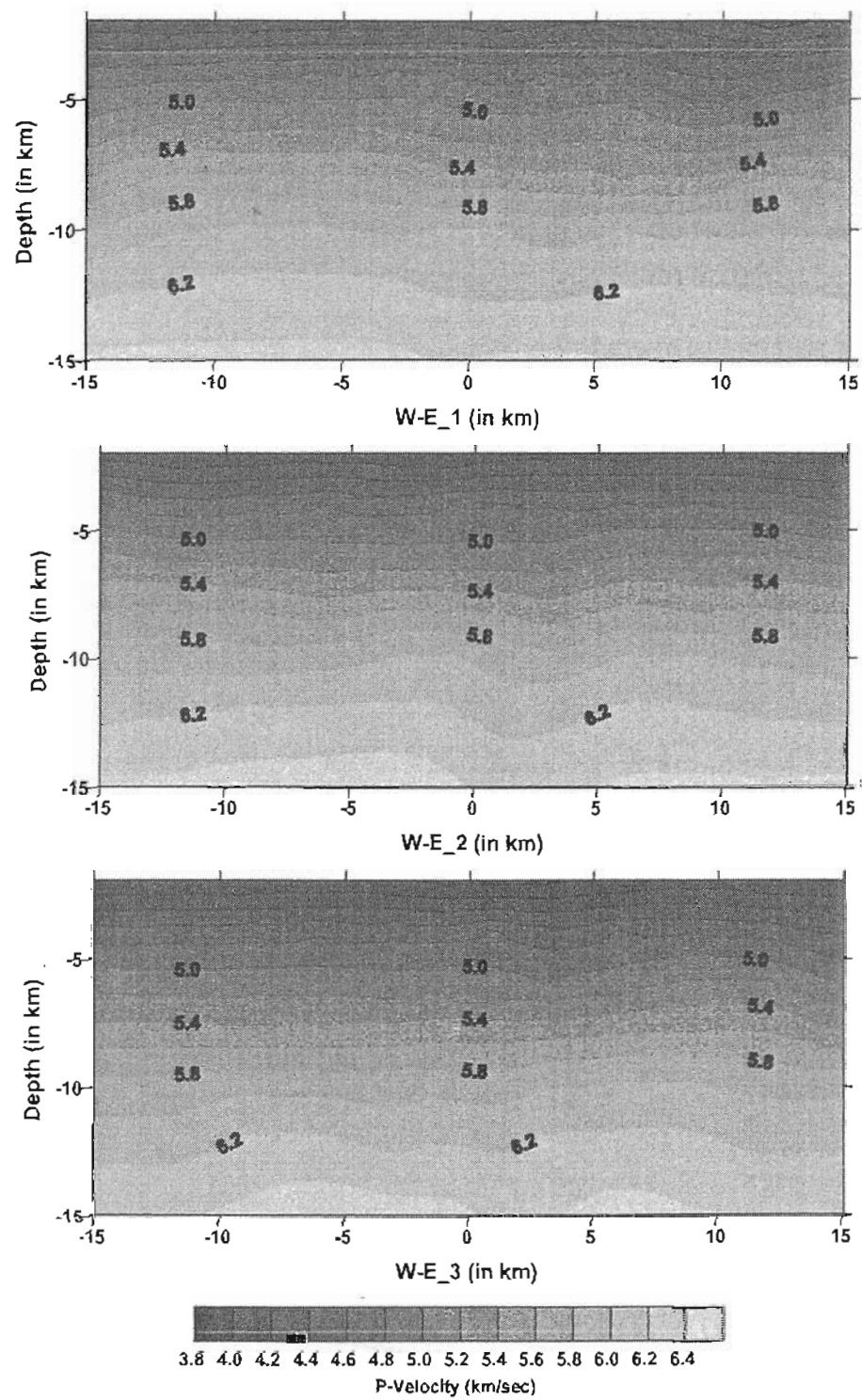


Figure 5a. The velocity distribution is shown, along the cross-sections of Figure 3, to the S-N directions.

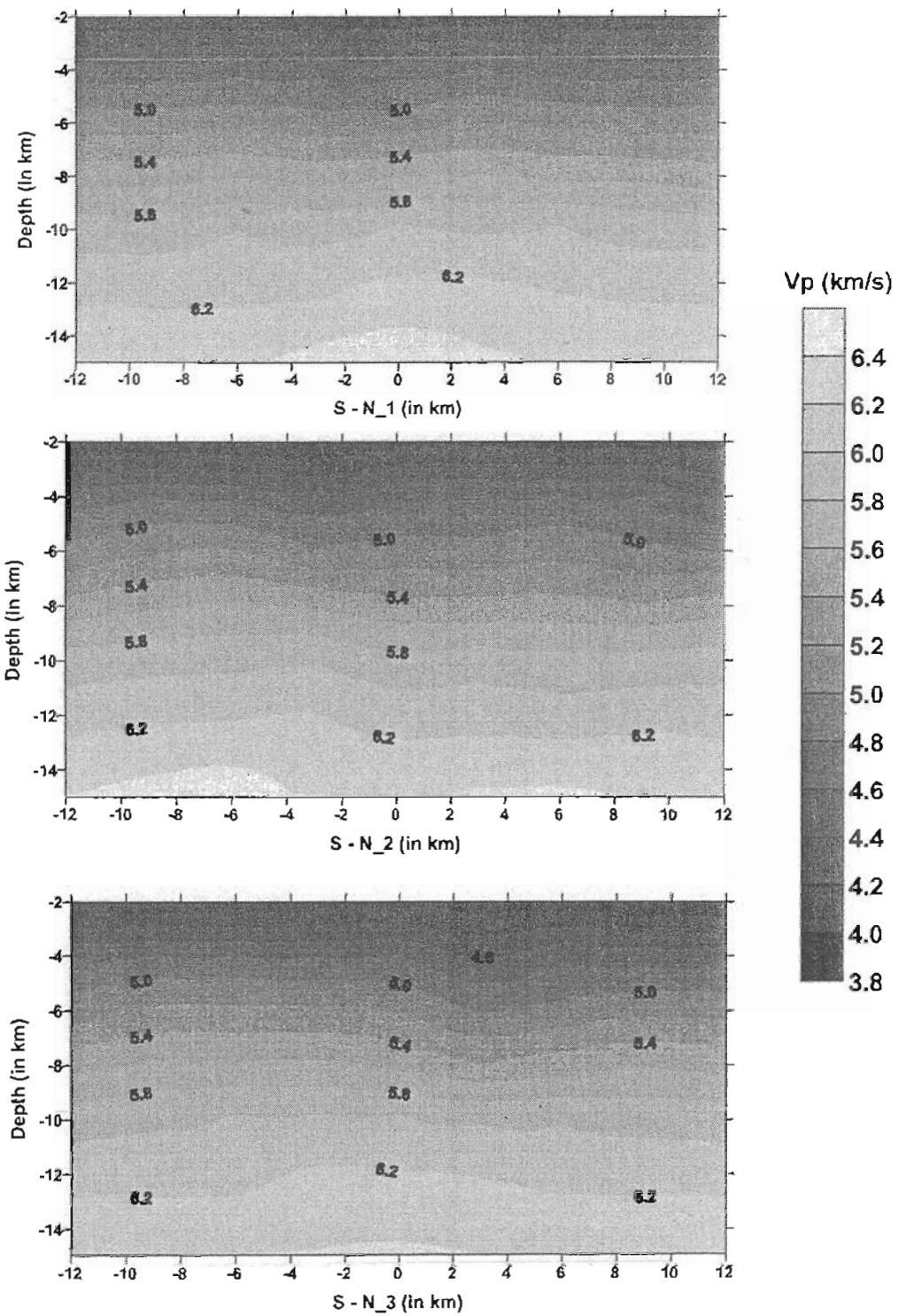


Figure 5b. The velocity distribution is shown, along the cross-sections of Figure 3, to the W-E directions.

At the depth of 2 km, an extended low velocity area covers the most the epicentral region. The velocity ranges from 3.88 to 4.12  $\text{kms}^{-1}$ . The low velocities at this depth seem to be typical for the sedimentary basins like those of the investigated region. At the depth of 4 km, the velocity distribution seems to be rather homogeneous in the whole region. The velocity ranges from 4.56 to 4.82  $\text{kms}^{-1}$ . In general at shallow depths (less than 4 km) a gradual vertical increase of the velocity is observed, without any sharp variation. On the contrary, the lateral variation of the velocity seems to be affected from the geological regime of the region. Low velocities are predominant beneath the sedimentary basins of Thriassio and Athens, while higher velocities are detected beneath the mountains of Parnes and Penteli (Figure 5).

The situation changes at the depth of 6 km. The velocity ranges from 4.96 to 5.22  $\text{kms}^{-1}$  and both vertical and lateral velocity variations are sharply pronounced. Relatively low velocities (about 5.00  $\text{kms}^{-1}$ ) cover the most part of the aftershock area. At the depth of 8 km, the velocity ranges from 5.36 to 5.62  $\text{kms}^{-1}$ . Like in the previous layer, two spots of low velocity zone are predominant in the aftershock area (Figure 5). The same situation exists at the depth of 10 km. Relatively low velocities cover the epicentral part of the investigated region, while a higher velocity zone is determined in the central part of Attiki, almost coinciding with the transition between the Pelagonian and Attico-Cycladic massifs (Figures 4 and 5)

The velocity distribution as determined at the two other layers (at the depths of 12 and 15 km) should be examined carefully. The results seem to be unstable and disputable due to the lack of deeper events and therefore the small number of seismic rays penetrating at these layers.

In general, the results are in good agreement with those of other investigators [10, 27], which investigated the tomographic structure of the region, using micro-earthquake data from other networks installed in the region.

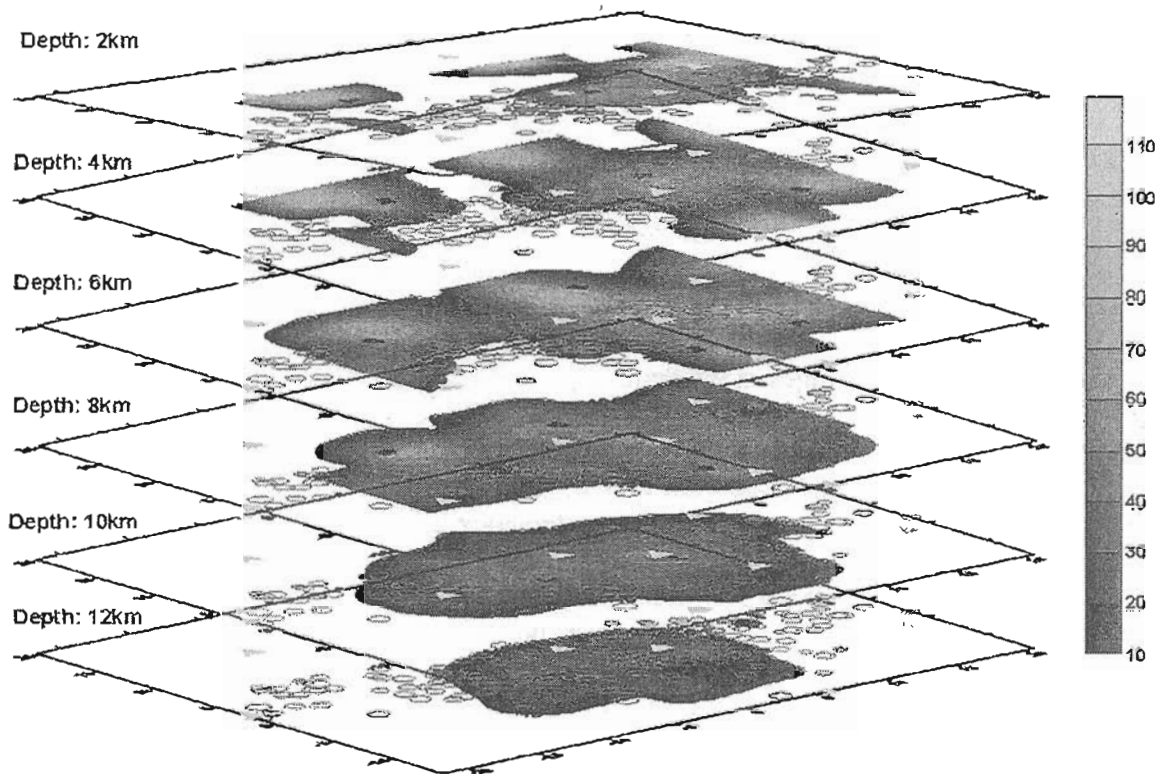


Figure 6. The number of hits at each layer of the region is shown.

## References

1. Galanopoulos, A.G. (1953) Katalog der Erbeben in Griechland für die Zeit von 1879 bis 1892. *Ann. Geol. Pays Hellen.*, 5, 144–229.
2. Galanopoulos, A.G. (1960) Greece: A Catalogue of shocks with  $I_0 > VI$  or  $M > 5$  for the years 1801–1958. *Seism. Lab. Univ. Athens*.
3. Ambraseys, N.N. (1994). Material for the investigation of the seismicity of Central Greece. *Historical Investigation of the Seismicity of European Earthquakes*, Albin, P. and A. Moroni (eds), 2, 1–10.
4. Ambraseys, N.N. and Jackson A. (1997) Seismicity and strain in the Gulf of Corinth (Greece) since 1694. *J. Earth. Eng.*, 1, 433–474.
5. Papazachos, B.C. and K. Papazachou (1997) The Earthquakes of Greece, *Ziti Publ., Thessaloniki*, pp 304.
6. Papadopoulos, G.A., Vassilopoulou, A. and Plessa A. (2000) A Catalogue of Historical Earthquakes for Central Greece: 480 B.C.–1910 A.D. *Institute of Geodynamics, National Observatory of Athens*, Publ. No 11.

7. Papadopoulos, G.A., Drakatos, G., Papanastassiou, D., Kalogeras, I. and Stavrakakis G. (2000) Preliminary Results about the Catastrophic earthquake of 7 September 1999 in Athens, Greece. *Seism. Res. Lett.*, 17, N. 3, 318–329.
8. Papanastassiou, D., Stavrakakis, G., Drakatos, G. and Papadopoulos G. (2000) The Athens, September 7, 1999, Ms=5.9, earthquake: first results on the focal properties of the main shock and the aftershock sequence. *Ann. Geol. Pays Hellen.*, 38 (B), 73- 88.
9. Stavrakakis, G.N., Chouliaras, G. and Panopoulou G. (2000) Seismic source parameters for the Athens earthquake on September 7, 1999, from a new telemetric broad band seismological network in Greece. *Ann. Geol. Pays Hellen.*, 38 (B), 15- 28.
10. Stavrakakis, G., Makris, J. and J. Staecker (2000) Aftershock properties of the Athens earthquake of Sep. 7, 1999, based on a dense digital seismological array. *Abstract, Proc. XXVII Ge. ASS. ESC, 10 – 15 September 2000, Lisbon (Portugal)*, p. 36.
11. Papadimitriou, P., Kaviris, G., Voulgaris, N., Kassaras, I., Delibasis, N. and K. Makropoulos (2000) The September 7, 1999 Athens earthquake sequence recorded by the CORNET network: Preliminary results of source parameters determination of the main shock. *Ann. Geol. Pays Hellen.*, 38 (B), 29-40.
12. Tselentis, G-A and Zahradnik, J. (2000) Aftershock monitoring of the Athens earthquake of 7 September, 1999. *Seism. Res. Lett.*, 71, 330–337.
13. Voulgaris, N., Kassaras, I., Papadimitriou, P. and Delibasis N. (2000) Preliminary results of the Athens September 7, 1999 aftershock sequence. *Ann. Geol. Pays Hellen.*, 38 (B), 51- 62.
14. Spakman, W. (1986) Subduction beneath Eurasia in connection with the Mesozoic Tethys. *Geol. Mijnbouw.*, 65, 145–153.
15. Spakman, W., Wortel, M.J.R. and Vlaar N.J. (1988) The Hellenic subduction zone: a tomographic image and its dynamic implications. *Geophys. Res. Lett.*, 15, 60-63.
16. Drakatos, G. and Drakopoulos, J. (1991) 3D velocity structure beneath the crust and upper mantle of the Aegean sea region. *Pure and Appl. Geophysics*, 135, 401–420.
17. Papazachos, C.B., Hatzidimitriou, P.M., Panagiotoopoulos, D.G. and Tsokas, G.N. (1995) Tomography of the crust and upper mantle in south-east Europe. *J. Geophys. Res.*, 100 (B7), 12405–12422.
18. Melis, N. and Tselentis, G-A. (1998) 3-D P-wave velocity structure in western Greece determined from tomography using earthquake data recorded at the University of Patras Seismic Network (PATNET). *Pure Appl. Geophys.*, 152, 329–348.
19. Rondoyanni, Th., Mettos, A., Galanakis, D. and Georgiou Ch. (2000) The Athens earthquake of September 7, 1999: its setting and effects. *Ann. Geol. Pays Hellen.*, 38 (B), 131-144.
20. Pavlides, S., Papadopoulos, G.A. and Ganas A. (1999) The 7<sup>th</sup> September, 1999 unexpected earthquake of Athens: Preliminary results on the seismotectonic environment. *Proc. 1<sup>st</sup> Conference Advances in Natural Hazard Mitigation: Experiences from Europe and Japan, Athens 3-4 November, 1999*, 80–85.
21. Kissling, E., Ellsworth, W.L., Eberhart-Phillips, D. and Kradolfer U. (1994) Initial reference models in local earthquake tomography. *J. Geophys. Res.*, 99 (B10), 19635-19646.
22. Kissling, E. (1988) Geotomography with local earthquake data. *Rev. Geophys.*, 26, 659–698.
23. Thurber, C.H. (1983) Earthquake locations and three-dimensional structure in the Coyote Lake area, Central California. *J. Geophys. Res.*, 88, 8226–8236.
24. Eberhart-Phillips, D. (1986) Three-dimensional velocity structure in Northern California coast ranges from inversion of local earthquake arrival times. *Bull. Seism. Soc. Am.*, 76 (4), 1025–1052.
25. Eberhart-Phillips, D. (1990) Three-dimensional P and S velocity structure in the Coalinga region, California. *J. Geophys. Res.*, 95, 15343–15363.
26. Drakatos, G., Karantonis, G. and G. Stavrakakis (1997) P-wave crustal tomography of Greece with the use of an accurate two-point ray tracer. *Annali di Geofisica*, XL, 1, 25–36.
27. Drakatos, G., Melis, N., Papanastassiou, D., Karastathis, V., Papadopoulos, G. and G. Stavrakakis, (2002) 3-D velocity structure from inversion of local earthquake data in Attiki (Central Greece) region. *Natural Hazards*.